buildings

Article

Transforming Zeolite Tuff and Cigarette Waste into Eco-Friendly Ceramic Bricks for Sustainable Construction

Jamal Eldin F. M. Ibrahim [1], Mohamed A. Basyooni-M. Kabatas [2,3,4,*], Ferenc Móricz [5] and István Kocserha [1]

[1] Institute of Ceramics and Polymer Engineering, University of Miskolc, H-3515 Miskolc, Hungary; jamalfadoul@gmail.com (J.E.F.M.I.)
[2] Dynamics of Micro and Nano Systems Group, Department of Precision and Microsystems Engineering, Delft University of Technology, Mekelweg 2, 2628 CD Delft, The Netherlands
[3] Department of Nanotechnology and Advanced Materials, Graduate School of Applied and Natural Science, Selçuk University, Konya 42030, Turkey
[4] Solar Research Laboratory, Solar and Space Research Department, National Research Institute of Astronomy and Geophysics, Cairo 11421, Egypt
[5] Institute of Mineralogy and Petrology, University of Miskolc, H-3515 Miskolc, Hungary; ferenc.moricz@uni-miskolc.hu
* Correspondence: m.a.basyooni@gmail.com or m.kabatas@tudelft.nl

Abstract: The use of waste materials has gained attention as a sustainable approach in various industries. Cigarette waste, which is typically discarded as a non-recyclable material, poses a significant environmental challenge due to its toxicity and slow decomposition rate. However, by incorporating this waste into ceramic bricks, new approaches for waste management and resource utilization are explored. This research work provides a detailed evaluation of the possibility of utilizing natural zeolite tuff incorporated with cigarette waste to produce sustainable ceramic bricks. Uniform powders are produced by milling various combinations of zeolitic tuff and cigarette waste using a planetary ball mill. The substitution ratios ranged from 0% to 12% by weight of the zeolitic tuff, with increments of 2%. Ceramic discs were formed by dry pressing and then subjected to sintering at different heat treatment temperatures (950–1250 °C). The impact of the inclusion of cigarette waste on the microstructural and technical features of zeolite tuff-based ceramic bricks has been thoroughly investigated. The results of the experiments demonstrate that incorporating cigarette waste into the development of ceramic bricks leads to improved thermal insulation properties, with thermal conductivity ranging from 0.33 to 0.93 W/m·K. Additionally, these bricks exhibit a lighter weight in a range of 1.45 to 1.96 g/cm^3. Although the inclusion of cigarette waste slightly reduces the compressive strength, with values ranging from 6.96 to 58.6 MPa, it still falls within the acceptable range specified by standards. The inclusion of cigarette waste into zeolite tuff is an innovative approach and sustainable practice for reducing energy consumption in buildings while simultaneously addressing the issue of waste disposal and pollution mitigation.

Keywords: zeolite tuff; cigarette waste; dry compaction; thermal conductivity; compressive strength

check for updates

Citation: Ibrahim, J.E.F.M.; Basyooni-M. Kabatas, M.A.; Móricz, F.; Kocserha, I. Transforming Zeolite Tuff and Cigarette Waste into Eco-Friendly Ceramic Bricks for Sustainable Construction. *Buildings* **2024**, *14*, 144. https://doi.org/10.3390/buildings14010144

Academic Editor: Syed Minhaj Saleem Kazmi

Received: 6 December 2023
Revised: 3 January 2024
Accepted: 4 January 2024
Published: 6 January 2024

1. Introduction

The global issue of waste management has reached critical proportions, with landfills overflowing and the environment suffering the consequences of our excessive consumption [1–3]. The disposal of some waste materials such as cigarette waste presents a significant challenge due to their hazardous characteristics and the large volume generated by this widespread habit [4–6]. However, in recent years, an innovative approach has emerged, utilizing ceramic bricks to mitigate the environmental impact of cigarette waste. By incorporating cigarette waste into the ceramic brick production process, novel solutions are being developed to address waste management concerns while minimizing the harm caused by discarded cigarettes [7–9]. Cigarette smoking has been a common habit for centuries, with its popularity reaching alarming levels around the world. The production of tobacco has inevitably led to a substantial increase in cigarette waste. Each year, billions of cigarette butts are discarded, resulting in enormous environmental problems [10,11]. Cigarette filters, typically consisting of cellulose acetate, take decades to decompose and leach toxic chemicals into the environment [12]. This waste not only contaminates soil and water sources but also poses significant risks to wildlife and marine ecosystems [13,14]. This detrimental environmental impact of cigarette waste necessitates innovative solutions for its management. In recent years, significant research has been directed toward the utilization of cigarette waste as an effective pore-forming agent in fired clay brick-making [15]. The aim of these studies is to optimize and evaluate the thermal insulation characteristics of the produced bricks, seeking to significantly improve their ability to minimize heat transfer [16], thereby offering an effective solution for improving energy efficiency in the construction industry. By incorporating cigarette waste into the manufacturing process, researchers aim to introduce porous structures within the clay bricks. These pores serve as insulating air pockets, reducing the transfer of heat through the material and enhancing its thermal insulation capabilities [8]. The cigarette waste behaves as a pore-forming element, facilitating the creation of these desirable porous structures within the fired clay bricks. As reported by Kurmus et al. [17], the addition of cigarette butts to clay bricks not only contributes to improved thermal properties but also offers potential energy efficiency benefits, highlighting the potential for utilizing cigarette waste as a valuable resource in sustainable brick manufacturing processes.

Furthermore, alternative natural materials like zeolite tuffs exhibit significant potential as primary ingredients in the development of innovative construction materials [18,19]. Zeolite tuff is widely distributed across various regions worldwide and has generated attention as a prospective contender for construction, attributed to its exceptional stability and durability. Although the zeolite content may fall short for more sophisticated applications [20], zeolitic tuff is an excellent building material. It stands out as a dependable source of essential silica and alumina, which are components necessary for fired ceramic brick-making. Remarkably, these zeolitic tuffs can function as viable alternatives to traditional clay-based raw materials in the brick manufacturing process [21–23]. Emerging zeolite tuff as a raw material in brick production offers a sustainable alternative for the construction sector, owing to its plentiful availability and straightforward accessibility [24]. Research has indicated that incorporating zeolite tuff into fired ceramic brick production can yield remarkable improvements in their physical and mechanical attributes [25]. Erdogmus et al., who studied the effect of compaction pressure and sintering temperature on the compressive strength of the produced bricks based on natural zeolite, found that increasing the firing temperature from 900 °C to 1100 °C significantly boosted the compressive strength of zeolite bricks molded at 15 MPa pressure, escalating it from 7.1 MPa to an impressive 51.2 MPa [26]. Despite the recognition zeolitic tuffs have obtained as construction material, their potential as raw materials for the manufacturing of brick has largely remained untapped. By utilizing this potential, the construction sector can benefit from a sustainable and cost-effective alternative to traditional raw materials, reducing environmental impact while maintaining high-quality building materials. The motivation behind this study arises from the remarkable abundance of zeolite tuffs found in the Tokaj region in Hungary [27]. The existence of these vast, untapped reserves sparked curiosity and prompted the exploration of utilizing zeolite tuffs as fundamental components in the production of porous ceramic bricks. Remarkably, there was a notable absence of prior research exploring the development of ceramic bricks that incorporated both zeolite tuff and cigarette waste before this investigation. Recognizing this research gap, the authors embarked on this study with the belief that their findings would significantly contribute to the existing knowledge in this field, opening new avenues of research and practical applications.

The basic objective of this research is to examine the viability and practicality of employing zeolite tuff and cigarette waste (tobacco residue and cigarette ash) in the development of lightweight bricks. The focus of this research lies in the incorporation of cigarette waste into zeolite tuff, utilizing the dry pressing method to manufacture cost-effective bricks that meet international standards for material properties [27]. In order to bridge a gap in current research, the authors of this study undertake a thorough investigation of the interaction between cigarette waste and zeolite tuff under various temperature conditions and concentrations. Through a comprehensive examination of this behavior, the study aims to provide novel insights and valuable knowledge on this topic. The study examines the technological attributes of compressed and burnt bricks resulting from the heat treatment process, with particular emphasis on the impact of the mixture content and sintering temperature. Through this research, a new procedure for producing bricks is presented, showcasing the possibility of reutilizing waste materials in building materials and offering a sustainable solution to waste management as society strives for a circular economy and innovative solutions that contribute to a greener and more sustainable future.

2. Materials and Methods

2.1. Mixture Ratios and Synthesis Process

The natural zeolite tuff utilized in this study was sourced from a mine located in Tokaj, Hungary. As for the cigarette waste used as an additive, it was collected locally as waste material. The cigarette butts are removed and the reamended ash and tobacco residue are collected. The raw materials underwent a series of preparatory steps. Initially, 2 kg of natural zeolite tuff and 300 g of cigarette waste were milled using a planetary ball mill and sieved via a 200-mesh sieve to achieve a uniform particle size (Figure 1). Subsequently, the prepared powders were measured using a sensitive scale and mixed based on Table 1. The prepared mixtures are then subjected to milling in a planetary ball mill at 150 rpm for 15 min to ensure the homogeneity of the zeolite tuff/cigarette waste mixtures. The resulting powder mixtures were then compressed into specimens using a cylindrical mold with dimensions of 25 mm in diameter and 10 mm in thickness, applying a uniaxial pressure of 55 MPa at room temperature. The specimens were then de-molded. A total of 196 samples were produced, and 49 samples were made for each set. The prepared samples were then subjected to sintering in a laboratory electric kiln at four distinct temperatures: 950, 1050, 1150, and 1250 °C for a duration of 4 h (Figure 2). Seven samples of each composition set were fired at each sintering temperature. The firing procedure was conducted at a controlled heating speed of 30 °C/h. Eventually, the fired specimens underwent a gradual cooling process, naturally returning to room temperature within the confines of the oven. The study involved a comprehensive investigation by subjecting the samples to diverse firing temperatures, with the objective of exploring the relationship between the introduction of cigarette waste into the natural zeolite tuff mixture and the firing temperature. The primary focus was to analyze how these factors synergistically influenced the properties of the bricks, considering the variations in the mineralogical composition and firing conditions.

Table 1. Powder mixtures' proportions.

Sample Code	ZCW0	ZCW2	ZCW4	ZCW6	ZCW8	ZCW10	ZCW12
Zeolite tuff (wt%)	100	98	96	94	92	90	88
Cigarette waste (wt%)	0	2	4	6	8	10	12

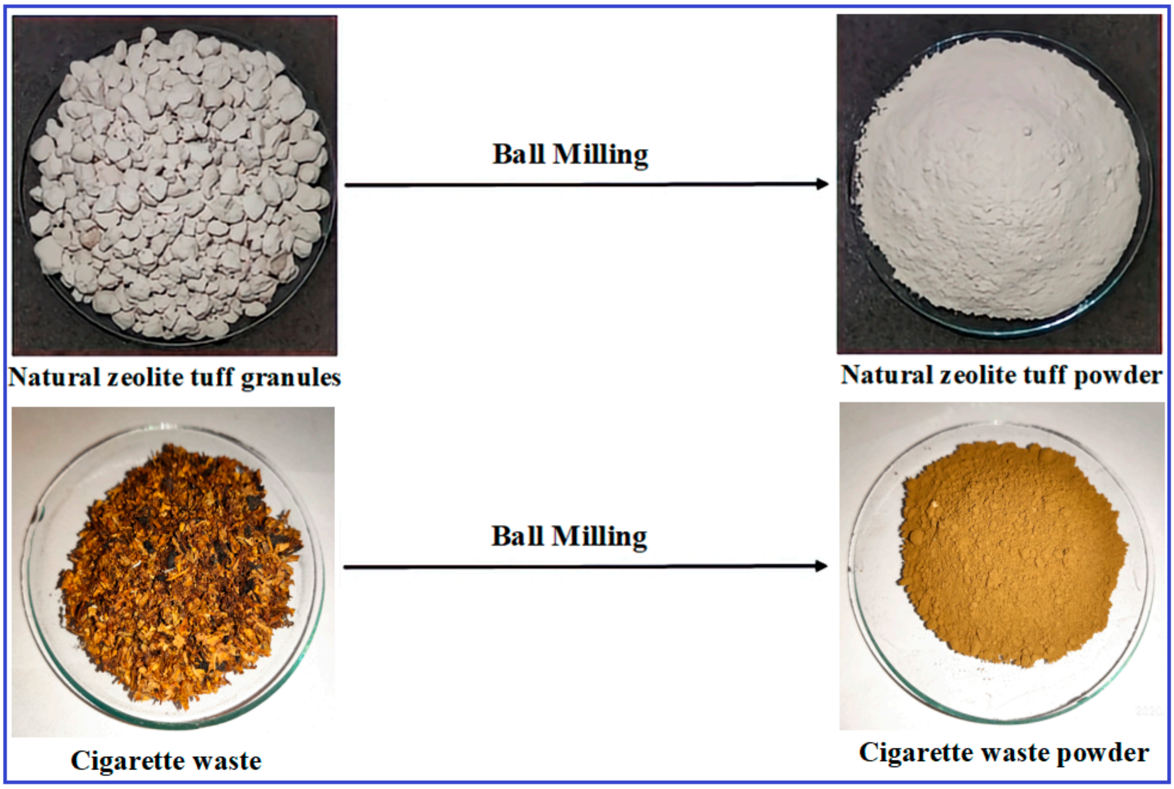

Figure 1. Basic raw materials prior to and after milling.

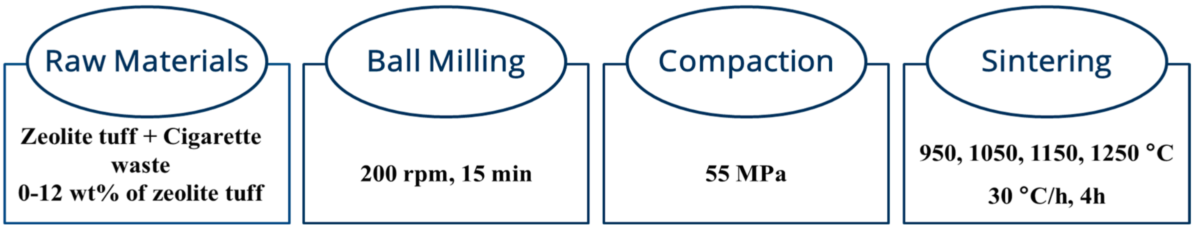

Figure 2. Process diagram of producing zeolite tuff/cigarette waste ceramic bricks.

2.2. Characterization Methods

A variety of characterization techniques were utilized to investigate the characteristics of the materials used in this research. An XRD analysis was performed using a highly precise Rigaku Miniflex II X-ray diffractometer fitted with a monochromator and CuKα radiation to analyze the phase composition in both the raw materials and sintered samples. The analysis was executed with a scanning speed of 1°/min, and the ICDD database was utilized as a reference. The raw powder's oxide content was examined through wavelength dispersive X-ray fluorescence analysis, employing the advanced capabilities of a Rigaku Supermini 200 WDXRF machine, Japan. This instrument utilized a Pd-tube with 200 W power, operating at 50 kV and 4 mA, with a 4 g pressed pellet configuration. The analysis was conducted using the ZSX software, ensuring a precise and comprehensive assessment of the oxide composition. The texture and morphology of the material particles were studied using a scanning electron microscope (SEM), specifically the Carl Zeiss model EVO MA10, operating in the secondary electron configuration. The SEM was integrated with an advanced (EDAX Genesis, USA) energy-dispersive X-ray analyzer for elemental investigation. Prior to analysis, a thin layer of gold was applied to the samples using a coating spray device to enhance reflection. The particle size analysis of the initial raw materials was evaluated using a tri-laser QUANTACHROME model CILAS715 analyzer, with distilled water serving as the dispersant. Using TG/DTA evaluation, the thermal behavior of the starting materials was determined through a Sestys evolution thermal analyzer, model 1750 SETARAM. Under a controlled oxygen atmosphere, the powdered samples underwent a gradual heating process at a constant rate of 10 °C per minute until reaching a temperature of 1200 °C. To evaluate the properties of the sintered bricks, such as their water absorption, apparent porosity, and the bulk density of the samples, Archimedes' principle, following the guidelines outlined in the ASTM C20 standard, was used as the measurement method. Compressive strength testing was conducted based on ASTM C67 using hydraulic universal testing equipment with a loading rate of 14 N/mm^2 per minute. Finally, the thermal conductivity analyzer (C-Therm TCi, Canada), utilizing the transient plane source (MTPS) method, was employed at an ambient temperature to determine the effusivity and thermal conductivities. This comprehensive range of analytical techniques provided a comprehensive overview of the materials' properties and heat transfer characteristics.

3. Results and Discussion

3.1. Starting Materials' Characterization Findings

3.1.1. XRD and XRF Analysis

The mineralogical examination shown in Figure 3 demonstrated that zeolite tuff comprises several primary constituents, namely smectite, clinoptilolite, illite/mica, and cristobalite, while quartz and calcite are present in smaller amounts, as indicated in Table 2. The XRF examination of the zeolite tuff's oxide compositions, reported in Table 3, revealed a substantial presence of silica, followed by alumina, and relatively smaller quantities of other oxides, such as calcium oxide, iron oxide, magnesium oxide, potassium oxide, and sodium oxide.

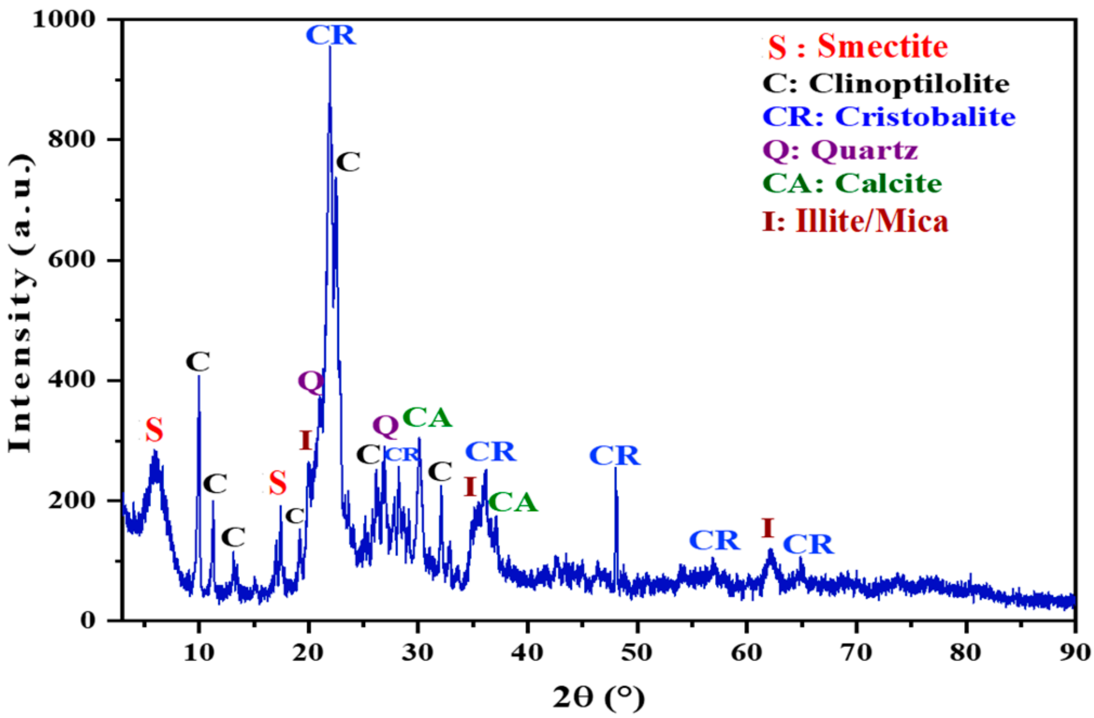

Figure 3. XRD graph of zeolite tuff.

Table 2. Phase content of zeolite tuff taken from XRD analysis.

Raw Materials	Phase Content					
	Clinoptilolite	Cristobalite	Illite/Mica	Smectite	Quartz	Calcite
Zeolite tuff	29.26	28.58	18.98	2.19	2.62	2.62

Table 3. Oxide composition of zeolite tuff taken from XRF analysis.

Raw Materials	Oxide Content								
	SiO_2	Al_2O_3	K_2O	Na_2O	Fe_2O_3	CaO	MgO	Others	LOI
Zeolite tuff	70.66	12.95	2.46	0.55	1.66	1.38	0.87	0.55	8.82

The examination of the cigarette waste (tobacco residue and cigarette ash) using X-ray diffraction, as depicted in Figure 4, revealed the presence of distinct crystalline phases including quartz (SiO_2), sylvite (KCl), and calcite ($CaCO_3$). XRD and XRF examinations offer detailed information about the crystalline composition of the raw materials, shedding light on the presence of these specific mineral phases within the examined samples.

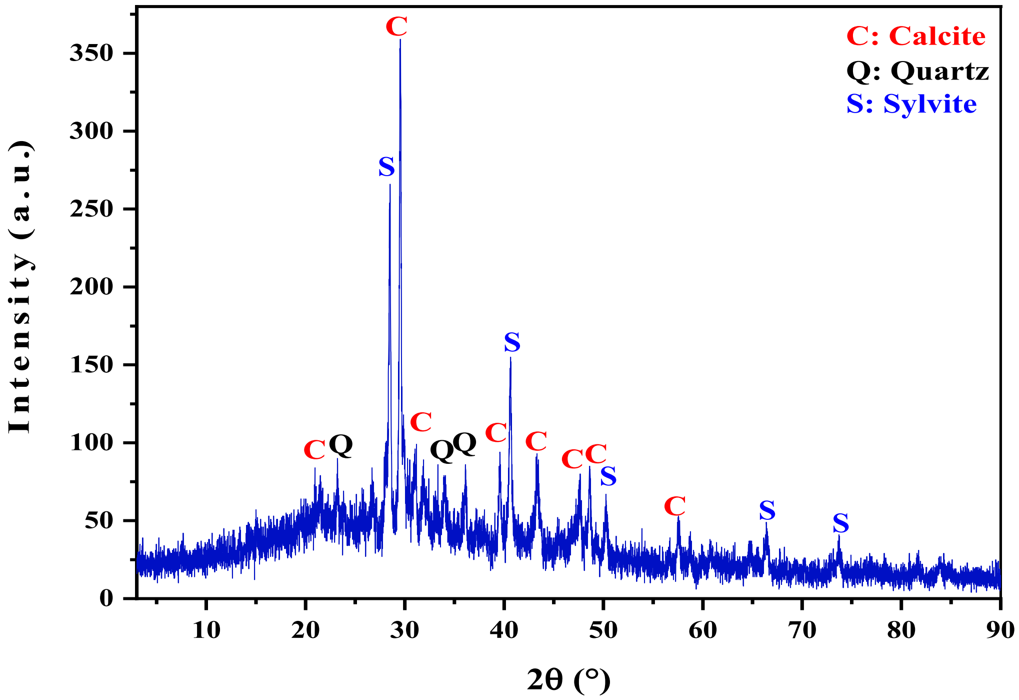

Figure 4. XRD diffractogram of cigarette waste.

3.1.2. SEM Examination of Raw Materials

Figure 5a displays SEM micrographs of the zeolite tuff, revealing distinctive characteristics. Notably, the existence of accumulated small particles is observed, forming lamellar layers with an uneven shape. These lamellar plates exhibit a tendency for smaller particles to adhere to larger ones or cluster together to form agglomerates. Moreover, the micrographs provide visual confirmation of a wide particle size distribution within the zeolite tuff. This visual evidence further supports the understanding of the particle size characteristics of the zeolite tuff.

Figure 5b showcases the SEM image of the cigarette waste, providing a visual representation of its particle morphology. The image reveals the presence of irregular and plate-like particles characterized by relatively larger sizes. This observation highlights the diverse and non-uniform nature of the particles comprising the cigarette waste.

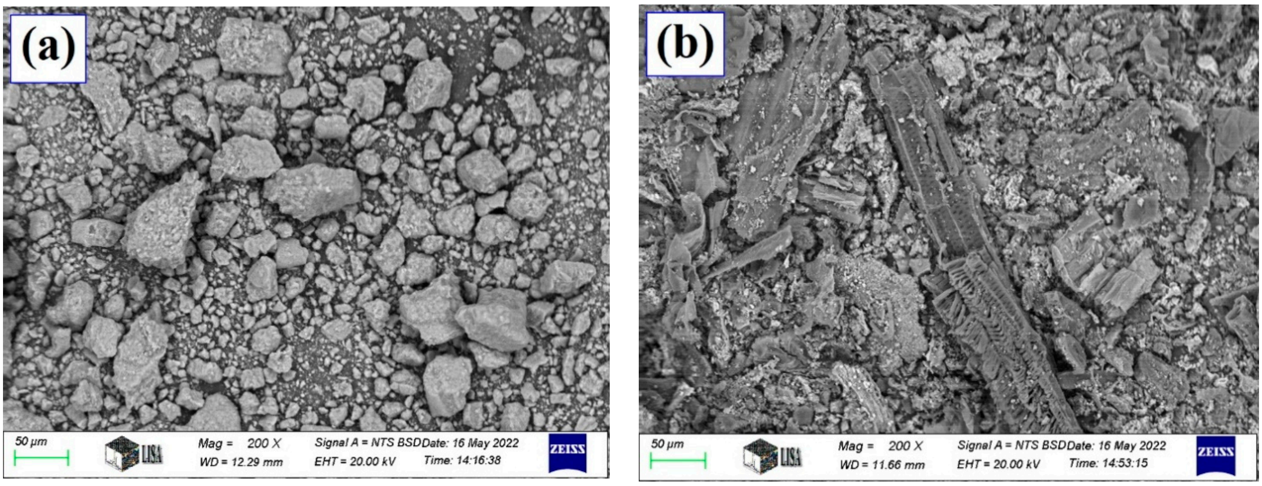

Figure 5. SEM photos of (**a**) zeolite tuff and (**b**) cigarette waste.

3.1.3. EDS Examination of Raw Materials

The EDS examination conducted on the zeolite tuff is shown in Figure 6a. It validates that the basic composition of the zeolite tuff is predominantly silica, accompanied by the existence of aluminum and various impurities. These results are consistent with the quantitative XRD measurements and XRF analysis illustrated in Table 2, where the silica is classified as the predominant constituent of the zeolite tuff.

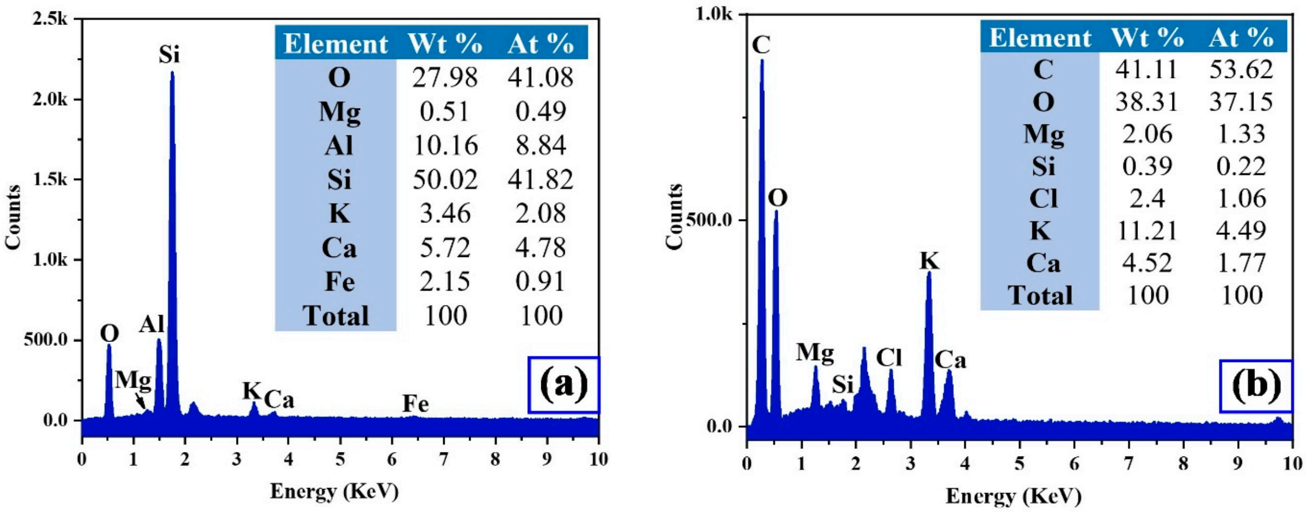

Figure 6. EDS patterns of (**a**) zeolite tuff and (**b**) cigarette waste.

The average EDS analysis of cigarette waste (Figure 6b) is carried out from a lower magnification image since it is a heterogeneous material. It is feasible to ascertain the predominant element in the composition, which is carbon. This is then followed by the presence of potassium and calcium. Furthermore, trace quantities of magnesium, chlorine, and silicon were detected. These specific substances are frequently found in plants, reinforcing their expected presence in cigarette waste. The EDS analysis not only provides valuable insights into the composition but also serves as a key resource for gaining a comprehensive understanding of the material's makeup.

3.1.4. Particle Size Distribution

The particle size distribution investigation of the zeolite tuff and the cigarette waste is exhibited in Figure 7. Notably, it is evident from the graph that the zeolite tuff exhibits relatively smaller particle sizes in comparison to the cigarette waste. Specifically, all the particles in the zeolite tuff fall below the 100 μm threshold, while approximately 9% of the cigarette waste particles exceed this size. The zeolite tuff exhibited a mean particle size, referred to as D50, of 16.6 μm, while the cigarette waste displayed a slightly larger average particle size of 18.15 μm. This variance in particle sizes can potentially facilitate the close-packing of the mixture. The particle size distribution analysis provides valuable insights into the range and average sizes of particles in both zeolite tuff and cigarette waste, aiding in the understanding of their physical characteristics and potential interactions.

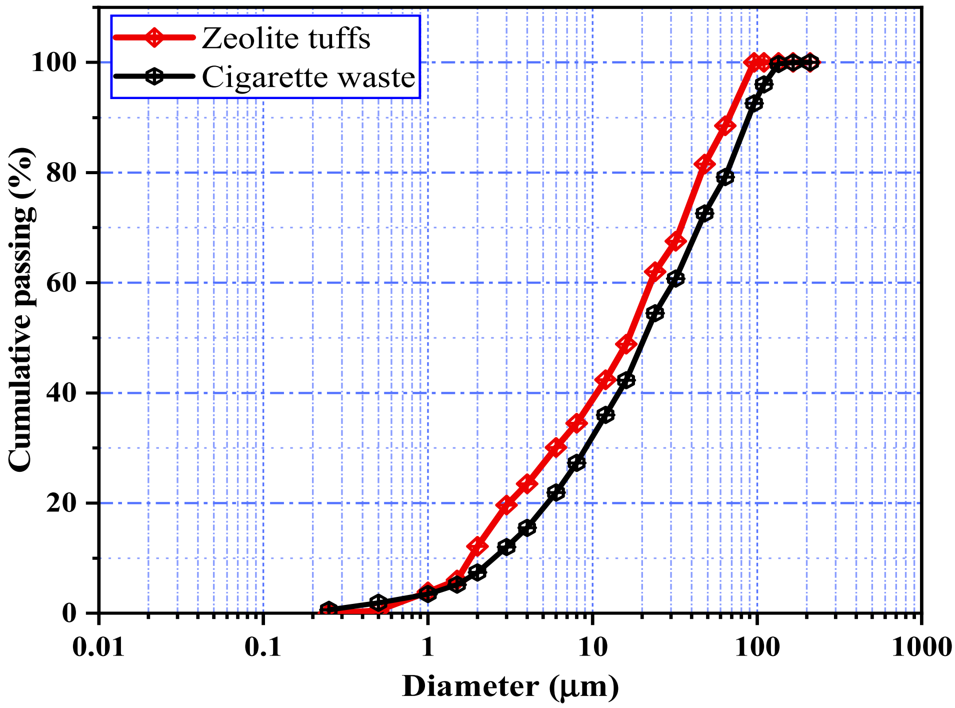

Figure 7. The particle size analysis for the zeolite tuff and cigarette waste.

3.1.5. Thermal Properties of Initial Raw Materials

The TG-DTG analysis provides valuable insights into the thermal decomposition behavior of the raw materials, shedding light on the different components and their respective contributions to weight loss. Based on the findings acquired from the TG-DTA curves, as depicted in Figure 8a, the zeolite tuff exhibited consistent behavior throughout the heating process, with three distinct events observed. Firstly, a mass loss of 5 wt% was observed between 30 and 292 °C, primarily ascribed to the moisture removal [28]. This was evidenced by a tiny endothermic peak at around 111 °C. Secondly, a mass loss of 2 wt% occurred between 292 and 541 °C. Within this temperature range, a significant exothermic peak was recorded at 340 °C, corresponding to the ignition of organic matter. Additionally, an endothermic peak was observed at a temperature of 523 °C, designating the removal of the crystalline water of the aluminosilicate compound and resulting in a 2% weight loss. Lastly, a 2 wt% mass loss between 541 and 797 °C was attributable to the carbonates' breakdown and subsequent CO_2 emission [29]. The TG-DTA analysis provides valuable insights into the thermal behavior and decomposition processes of zeolite tuff, aiding in the understanding of its properties and potential applications.

Figure 8b illustrates the TG-DTA patterns derived from the combustion of cigarette waste and its constituents within a temperature range of 30–1200 °C/min. A notable observation is that the components of cigarette waste exhibit characteristic decomposition behaviors in terms of weight loss. The sample exhibits four distinct mass-loss regions. The initial weight loss of 5.1% occurs at 30–111 °C, primarily assigned to the evaporation of absorbed moisture. An observable signal in the form of a minor endothermic peak, precisely centered at 86.2 °C, provided clear evidence of this phenomenon. The main decomposition region, comprising 41 wt% of the weight loss, is observed in the temperature of 111–322 °C. This was indicated by a large exothermic peak at 278 °C. This weight loss is primarily due to the breakdown of organic volatiles that exist in cigarette waste, such as tar and nicotine components. The last weight loss of 31.4% occurs at 322 to 826 °C related to an exothermic peak at 418 °C, resulting from the breakdown of unfired tobacco. As a result, unburned components persist as a solid remaining portion, manifesting as distinct carbon black particles.

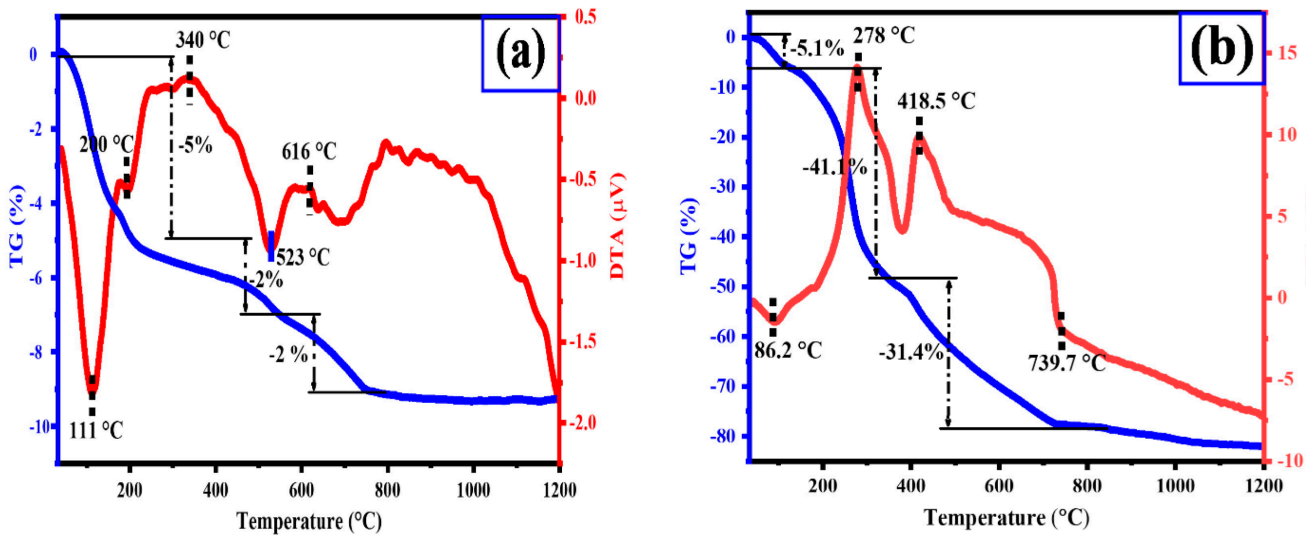

Figure 8. TG/DTA graphs of (**a**) zeolite tuff and (**b**) cigarette waste.

3.2. Characterization Outcomes of the Developed Specimens

3.2.1. Dimensional Characteristics of the Heat-Treated Specimens

Bricks made from zeolite tuff incorporated with varying percentages of cigarette waste were produced as depicted in Figure 9. Notably, zeolite tuff-based bricks were able to accommodate up to 12% of the cigarette waste without experiencing any cracks throughout the manufacturing. The samples sintered at variable temperatures exhibited a whitish appearance, accompanied by noticeable volume shrinkage which was determined by subtracting the sample's volume after sintering from the volume before sintering. The final coloration of the ceramic materials can exhibit a diverse spectrum, encompassing dark, red, and white hues. This color variation primarily stems from the presence of Fe_2O_3, as well as other components such as TiO_2 and CaO. Notably, when the Fe_2O_3 ratio remains under 3%, ceramic materials can be classified as light-firing clays. This result is in line with the XRF analysis which shows a low content of Fe_2O_3 in the raw materials. Furthermore, by controlling the total proportion of Fe- and Ti-bearing components that remain under 6% in the ceramic specimens, pale white products can be achieved [30]. Furthermore, the fired brick showed an alteration in color at different temperatures. This could be due to the change in the content of the different phases. These findings highlight the ability to incorporate cigarette waste into zeolite tuff bricks while maintaining structural integrity and demonstrate the influence of different oxide contents on the fired color and characteristics of the resulting ceramic materials.

Figure 9. Produced bricks at different temperatures.

3.2.2. XRD Investigations

Figure 10 showcases the XRD patterns of an unfired ZCW6 brick and a ZCW6 brick fired at different temperatures (950 to 1250 °C). In the unfired brick, the major phases identified were smectite ($(Na,Ca)_{0.33}(Al,Mg)_2Si_4O_{10}(OH)_2 \bullet n(H_2O)$), clinoptilolite ($(Na_2,K_2,Ca)_3Al_6Si_{30}O_{72}\cdot 24H_2O$), illite/mica ($K_{0.65}Al_2[Al_{0.65}Si_{3.35}O10](OH)_2$), and cristobalite ($SiO_2$), while minor phases included quartz (SiO_2) and calcite ($CaCO_3$). The heat-treated zeolite tuff/cigarette waste bricks predominantly exhibited the crystalline phase of cristobalite with a minor phase of anorthite ($CaAl_2Si_2O_8$). The formation of anorthite phases is attributed to the physicochemical interaction of the molten mix, arising from the disintegration of smectite, clinoptilolite, illite/mica, and calcite. A decrease in the quartz content correlates with an increase in cristobalite quantity. Remarkably, the enhancement of the compressive strength of the specimens aligns with the formation of anorthite [31,32]. These findings shed light on the phase composition changes occurring throughout the firing process and the corresponding influence on the characteristics of the zeolite tuff containing cigarette waste bricks.

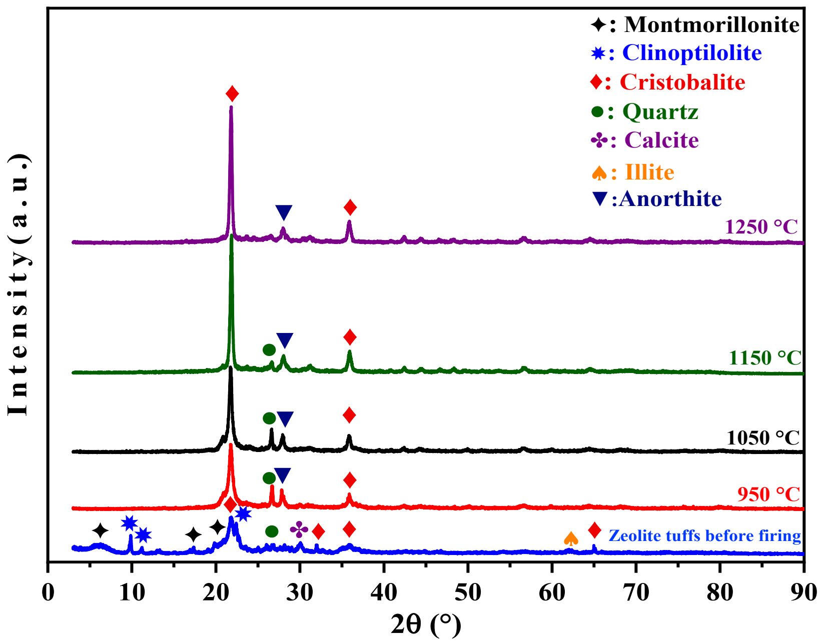

Figure 10. XRD graphs of the ZCW6 bricks sintered at various temperatures.

3.2.3. SEM Identification of the Fired Ceramic Bricks

The scanning electron images (Figure 11) present the morphological features and microstructural characteristics of the fractured surface of the ceramic bricks with varying compositions that were fired at 1050 °C. The SEM analysis consistently demonstrated a notable pattern: an increase in cigarette waste quantity corresponded to higher surface porosity and less developed bond structures. As a consequence, this yielded enhanced thermal insulation properties but weakened the compressive strength of the fired bricks. Consequently, this resulted in improved thermal insulation properties [33,34], while compromising the compressive strength of the fired bricks. The SEM photos align with the findings from the bulk density, apparent porosity, and water absorption tests, providing further support for the observed effects of cigarette waste on the overall structure and properties of the ceramic specimens.

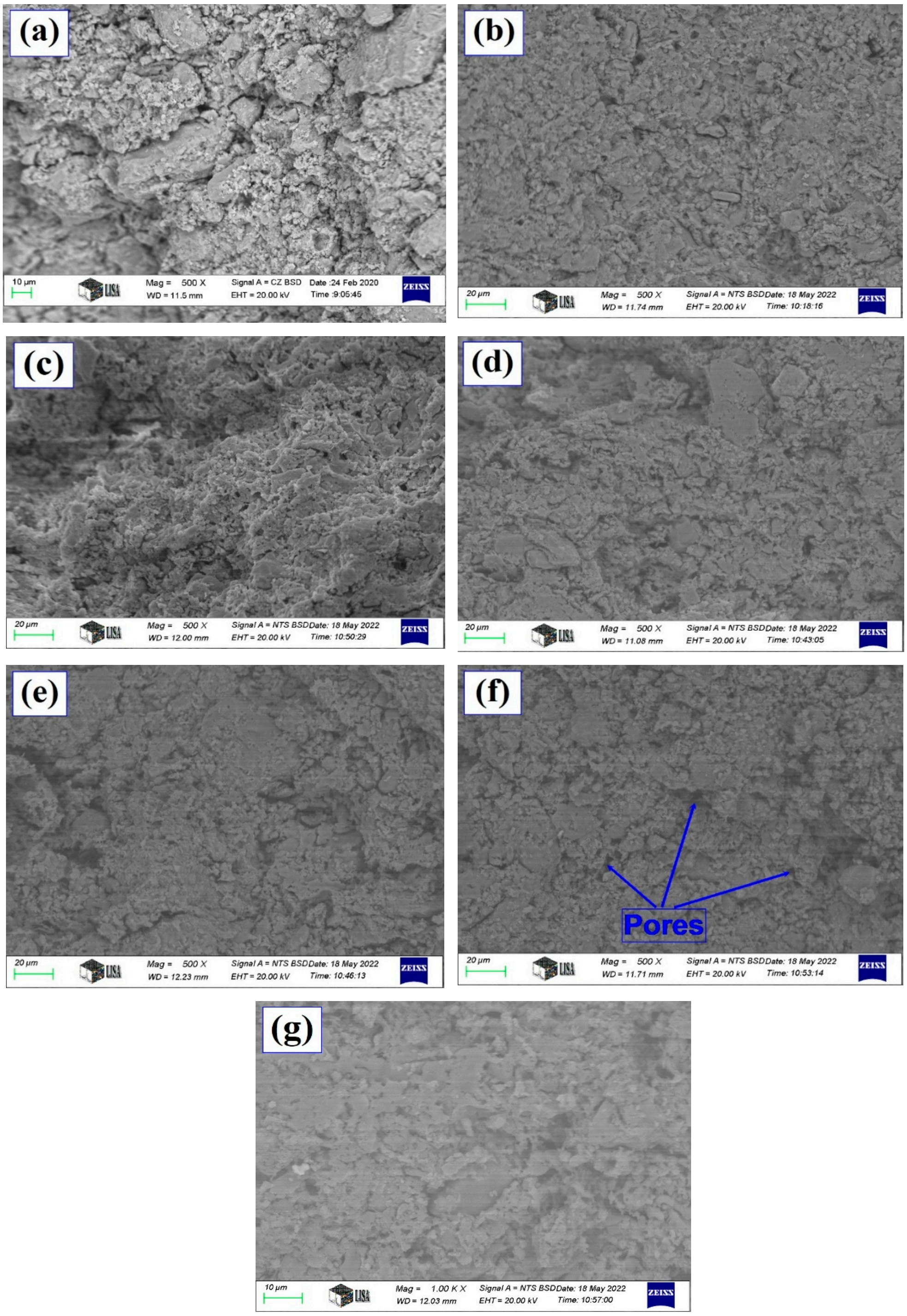

Figure 11. SEM photos of the prepared bricks: (**a**) ZCW0; (**b**) ZCW2; (**c**) ZCW4; (**d**) ZCW6; (**e**) ZCW8; (**f**) ZCW10 and (**g**) ZCW12 fired at 1050 °C.

3.3. Technical Attributes of the Ceramic Samples

3.3.1. Bulk Density

Figure 12 illustrates the density variations of the brick samples with various amounts of cigarette waste fired at different sintering temperatures. Notably, all the brick samples incorporating cigarette waste exhibit lower densities compared to the blank brick samples. The zeolite tuff bricks, when combined with cigarette waste, displayed bulk densities ranging from 1.45 g/cm^3 to 1.91 g/cm^3. In contrast, the control-fired zeolite tuff bricks, which were not mixed with cigarette waste and fired within the temperature of 950 to 1250 °C, exhibited comparable density values ranging from 1.63 g/cm^3 to 1.96 g/cm^3. The decrease in density observed in the bricks containing cigarette waste can be attributed to the higher porosity and volume shrinkage of these samples, which is consistent with previous research where a similar reduction in the density of clay bricks was reported with the inclusion of 10% rice husk RH [35]. However, it is noteworthy that the density significantly increases with the rise in temperature, ranging from 1.54 g/cm^3 to 1.81 g/cm^3 for bricks containing 6% cigarette waste as the sintering temperature is raised from 950 °C to 1250 °C. This rise in bulk density is an outcome of the densification processes and the effects of the firing temperature, as discussed in previous research works [36,37]. The rise in temperature promotes pore-filling and condensation events, leading to increased densification and a corresponding decrease in apparent porosity.

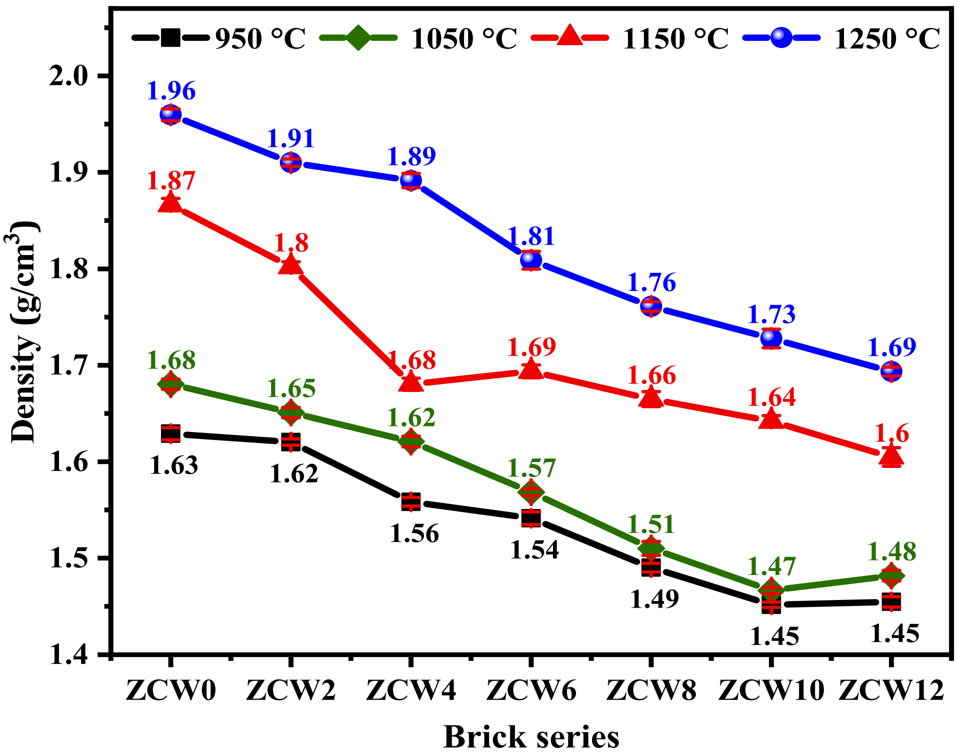

Figure 12. Density of the developed bricks under different sintering temperatures.

3.3.2. Apparent Porosity

The apparent porosity significantly influences the technical characteristics of the ceramic bricks. A rise in apparent porosity is normally associated with a decline in compressive strength, an increase in water absorption, and improved thermal insulation features [38,39]. Figure 13 illustrates the results of the apparent porosity for zeolite tuff bricks containing different percentages of cigarette waste. The findings indicate that apparent porosity increases with higher replacement percentages of cigarette waste. For instance, the porosity of the reference specimens (ZCW0) is 18%, which rises to 39.4% when 12% cigarette waste is included and sintered at 1050 °C. This rise in porosity can be attributed to the decomposition of cigarette waste during the sintering process. These results are consistent with similar studies conducted previously [40,41]. Porous bricks are valuable as insulation materials, particularly in applications requiring resistance to heat and cold. Conversely, increasing the sintering temperature leads to a reduction in the porosity due to the increased formation of the molten phase throughout the high-temperature sintering. This promotes the vitrification process and diminishes the internal porous connections, resulting in the improved strength of the bricks.

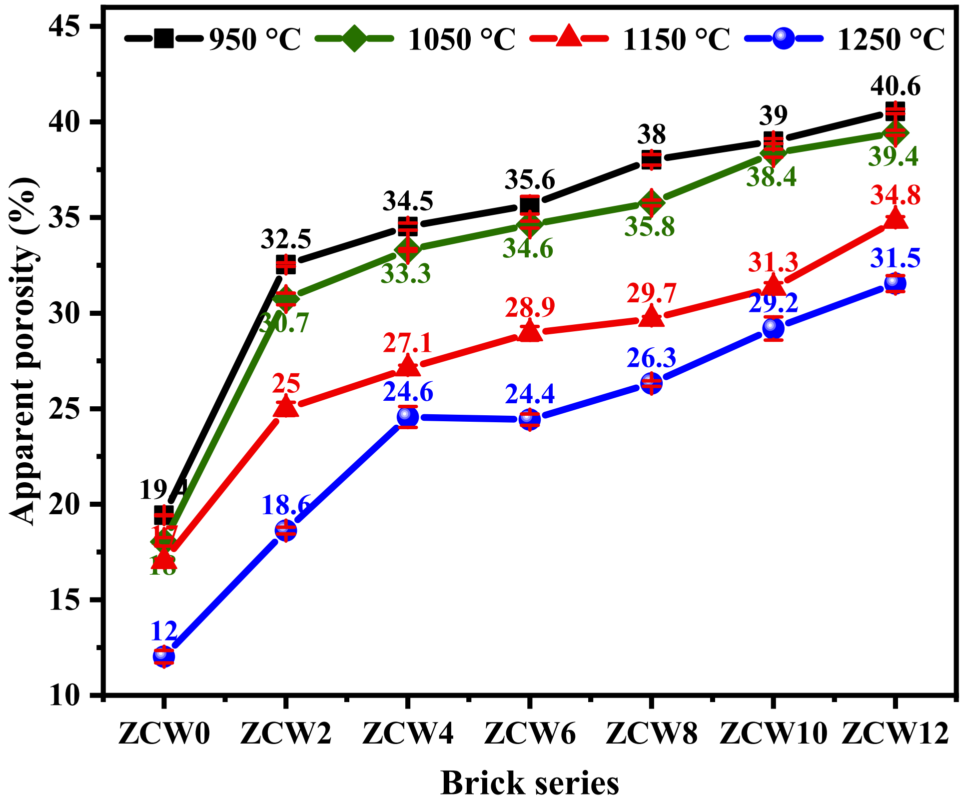

Figure 13. Apparent porosity of the developed bricks under different sintering temperatures.

3.3.3. Volume Shrinkage

The sintering process of the specimens is affected by the presence of flux materials and gaseous components, which affect volume shrinkage. Flux materials contribute to the formation of molten substances that fill in the gaps [42], while gaseous components release gases that expand the pores [43]. The dimensions of bricks with different compositions undergo variations due to shrinkage during the firing process at various temperatures, demonstrating their expansion and contraction behavior (Figure 14). Control samples at each temperature exhibit relatively lower volume shrinkage, ranging from 8.86% to 19.6%. However, the inclusion of 12% cigarette waste results in increased shrinkage, ranging from 13.1% to 30.9%. The combustion of cigarette waste generates gaseous expansion, leading to the formation of voids and capillaries within the zeolite tuff matrix at various scales. Nevertheless, as the sintering temperature rises, the shrinkage also increases. This can be attributed to the vitrification process, where the heating causes the formation of glassy layers within the ceramic body, bonding the zeolite tuff particles together [44].

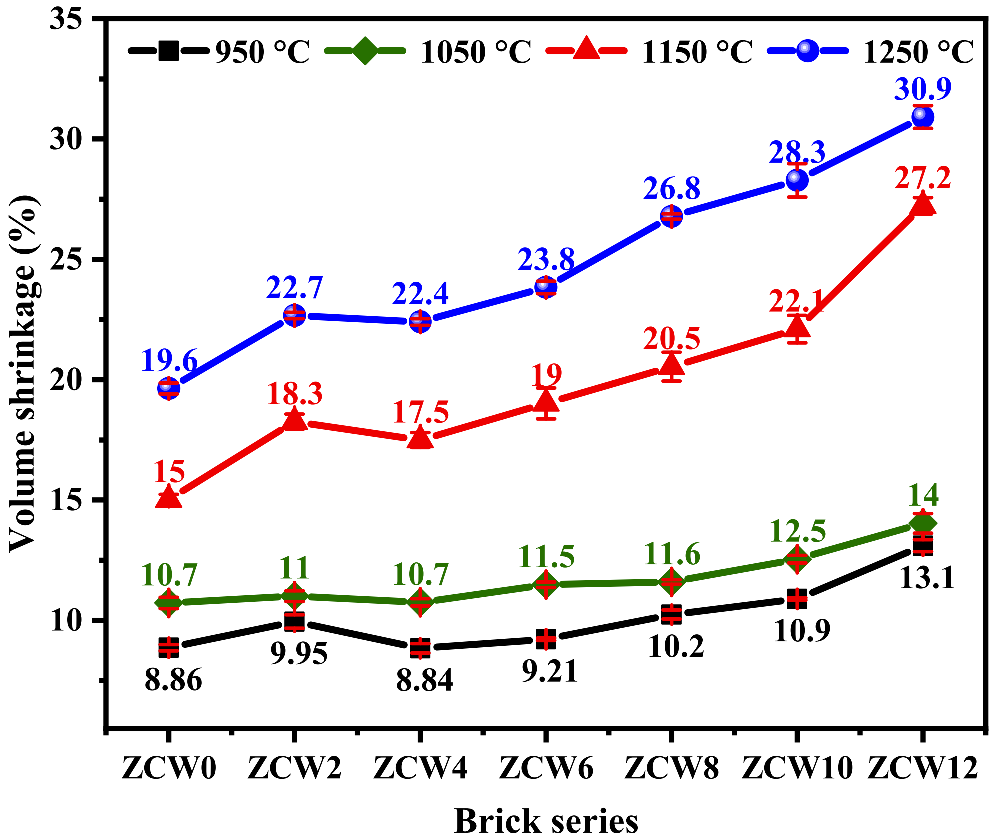

Figure 14. Volume shrinkage of the developed bricks under different sintering temperatures.

3.3.4. Water Absorption

Water absorption is a key element that directly impacts the life span of fired bricks. High water absorption can render bricks susceptible to weathering and chemical attacks [45,46]. Figure 15 illustrates the water absorption values of the zeolite tuff bricks with varying proportions of cigarette waste, fired at different temperatures. Water absorption is closely linked to open porosity, and both properties exhibit a similar trend. As the firing temperature increases, the water absorption of all compositions decreases, possibly due to the limited closure of the pores or a reduction in the interconnection between pores caused by the heat treatment. Conversely, water absorption rises with the inclusion of cigarette waste at the same firing temperature. The observed result aligns with the anticipated outcome, as the firing process effectively eliminates the organic matter that exists in cigarette waste. According to ASTM C62 standards, bricks are required to exhibit specific water absorption rates depending on the desired weathering resistance level. To ensure good resistance against severe weathering, it is essential that the water absorption rate remains below 17%. In situations with moderate weathering, the acceptable limit is established at 22%. Notably, in instances of negligible weathering conditions, there exists no specified upper threshold for water absorption [47]. Considering these criteria, bricks containing up to 6% cigarette waste and sintered at 1250 °C fall below the 17% limit. Meanwhile, the same samples sintered at lower temperatures (1150 °C, 1050 °C) meet the limit for moderate weathering. Bricks containing higher levels of waste materials could be well-suited for applications focused on insulation, where they are not exposed to direct contact with water.

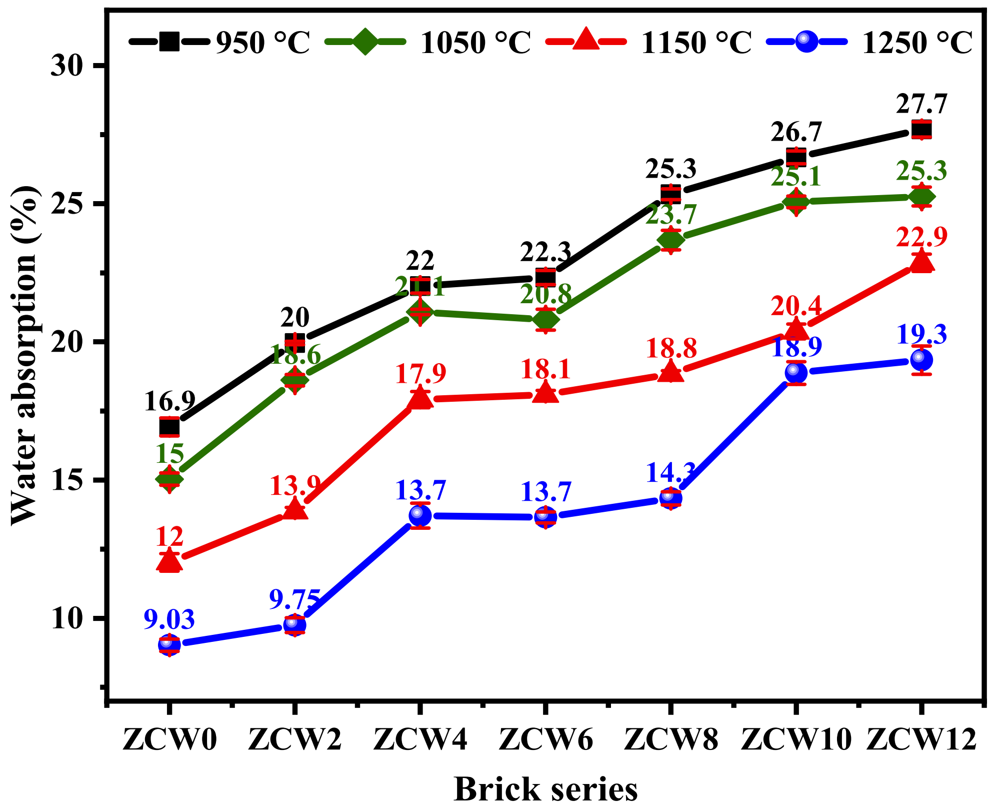

Figure 15. Water absorption of the developed bricks at different sintering temperatures.

3.3.5. Compressive Strength

Compressive strength is a major characteristic that judges the suitability of a material for use in building applications, serving as a reliable indicator of its quality [48]. Figure 16 illustrates the compressive strengths of different compositions at various firing temperatures. The findings indicate a consistent decline in the strength as the proportion of cigarette waste increases in the brick composition across all firing temperatures when compared to the reference samples. This can be ascribed to the higher porosity resulting from the decomposition of the carbonaceous matter present in the cigarette waste. These results are in line with previous research works on fired clay bricks [49,50]. The fired brick specimens exhibited a broad range of compressive strength, spanning from 6.9 MPa to 58.6 MPa. The reference bricks, subjected to sintering at a temperature of 1250 °C, exhibited the highest levels of compressive strength among all the tested samples, while the lowest values were determined in the ZCW12 bricks sintered at 950 °C. Notably, an evident decline in compressive strength was detected as the ratio of cigarette waste in the bricks increased from 2% to 12%, mainly due to the formation of pores within the material. However, as the temperature elevated from 950 to 1250 °C, a noticeable enhancement in the compressive strength of the bricks was observed, indicating an enhanced densification at higher temperatures facilitated by increased liquid phase formation and vitrification. The produced bricks in this study exhibited compressive strengths above 7 MPa, except for the samples containing 12% cigarette waste sintered at 950 °C, which displayed compressive strengths of 6.9 MPa. Consequently, these bricks can be deemed suitable for various construction applications, meeting the classification criteria for first-class or second-class bricks with crushing strengths exceeding 5 MPa and 7 MPa, respectively [51].

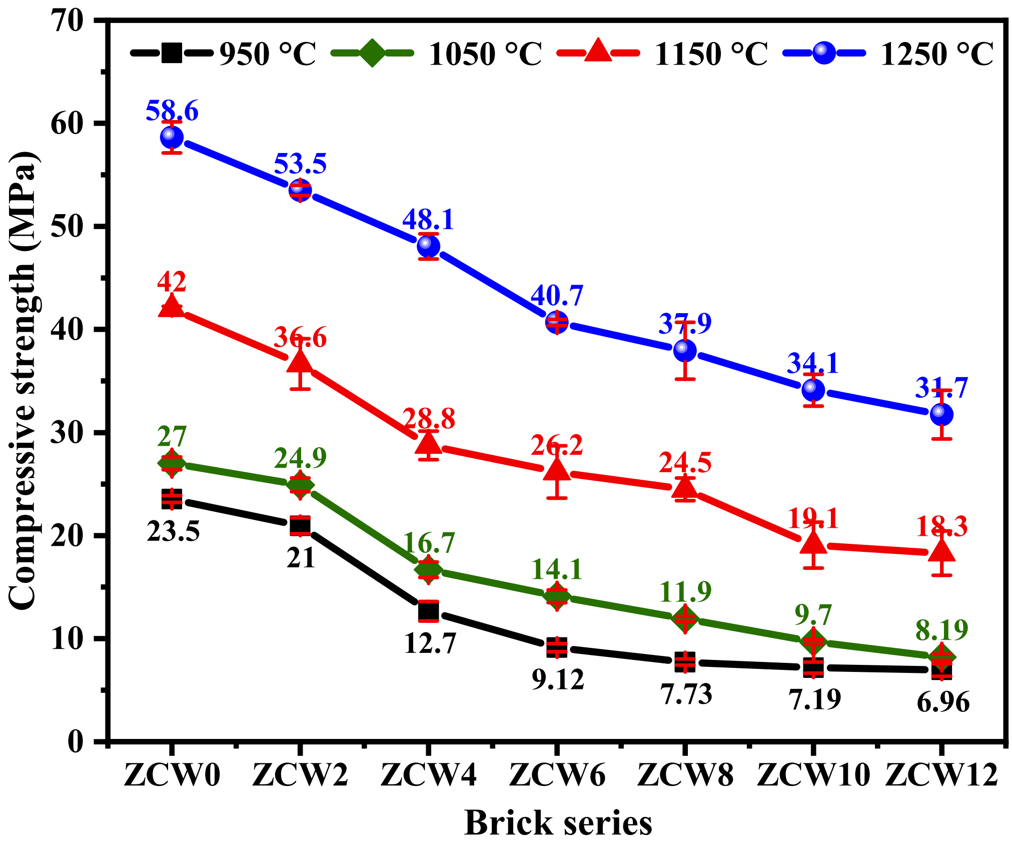

Figure 16. Compressive strength of the developed bricks under different sintering temperatures.

3.3.6. Thermal Conductivity

The thermal conductivity of the zeolite tuff bricks mixed with cigarette waste, after undergoing the firing process, is depicted in Figure 17. The control brick specimens, without cigarette waste, sintered at 950 °C, exhibited a relatively high thermal conductivity value, measuring approximately 0.53 W/m·K. Conversely, the bricks incorporating 12% cigarette waste, sintered at 950 °C, exhibited the most favorable thermal conductivity value, recording a value of about 0.33 W/m·K. This indicates a significant reduction in thermal conductivity by approximately 37.7% compared to the blank bricks. This aligns with previous studies where a similar reduction in thermal conductivity is observed due to the inclusion of marble waste as a pore-forming agent in the clay brick [52]. The porosity serves as a crucial factor in determining the thermal performance of clay bricks, as open pores are typically filled with air, acting as insulators and reducing thermal conductivity [53]. In addition to the influence of incorporating cigarette waste, the firing temperature also has a notable impact on the thermal conductivity. With increasing firing temperatures, thermal conductivity increases as well. For instance, upon sintering the ZCW6 samples at 950 °C, their thermal conductivity measured 0.42 W/m·K, and this value increased to 0.75 W/m·K after sintering the samples at 1250 °C. The high-temperature heat treatment process promotes the formation of a liquid phase and densification of the samples, thereby reducing the pore volume and porosity, ultimately resulting in an increase in thermal conductivity.

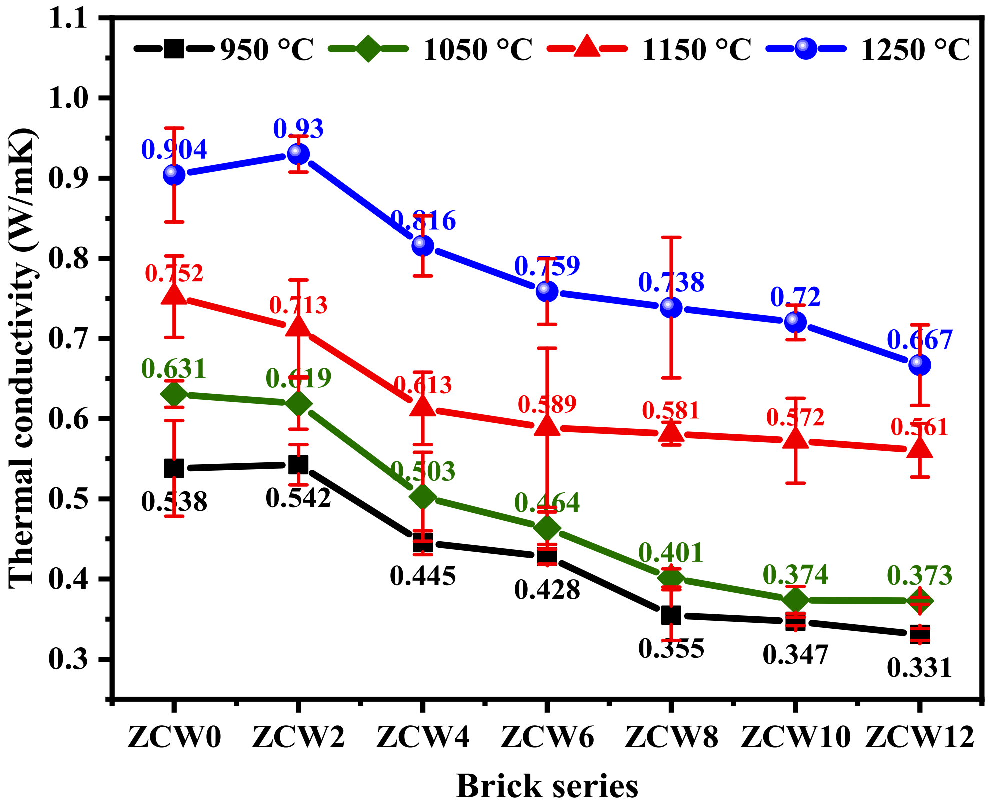

Figure 17. Thermal conductivity of the developed bricks under different sintering temperatures.

3.4. Comparison of the Findings of This Study with Those of Other Research in the Literature

Table 4 compares the findings from this research with those of various studies dedicated to exploring the utilization of waste materials in the creation of fired bricks. A clear pattern in these investigations indicates that the inclusion of waste materials often results in rising water absorption and porosity, accompanied by a reduction in compressive strength. However, this study's comparison with the data in Table 4 reveals the promising prospect of incorporating cigarette waste into natural zeolite tuff for brick manufacturing. This blend exhibits good qualities, especially in terms of its compressive strength and insulation properties, surpassing the outcomes of several studies listed in Table 3. This highlights the possibility inherent in combining natural zeolite tuff with cigarette waste, presenting a fascinating approach to innovative and sustainable brick production.

Table 4. An overview of the existing literature on fired bricks, highlighting key results in comparison to the main outcomes in this study.

Starting Raw Materials	Waste Added	Forming Technique	Sintering Temperature (°C)	Key Technical Characteristics				Ref.
				Water Absorption (%)	Density (g/m^3)	Thermal Conductivity (W/m·K)	Compressive Strength (MPa)	
Zeolite tuff	Cigarette waste	Dry pressing	950–1150	9.03–27.7	1.45–1.96	0.33–0.93	6.96–58.6	This work
Natural zeolite tuff	Aluminum dross	Dry pressing	950–1150	11.1–20.2	1.59–1.91	0.32–0.7	15–57	[54]
Natural zeolite	Eggshell	Dry pressing	950–1150	16.1–25.9	1.45–1.76	1.25–0.7	14.9–35.1	[55]
Glass powder	Poly-aluminum chloride slag	Semi-dry pressing	900–1100	23.5–26	1.56–1.6	–	5.6–9	[56]
Clay	Limestone waste	Dry pressing	900	–	1.31–1.9	–	6.9–15.8	[57]
Clay	Volcanic tuff	Dry pressing	900–1100	–	1.42–1.91	–	5–35.1	[22]

Table 4. *Cont.*

Starting Raw Materials	Waste Added	Forming Technique	Sintering Temperature (°C)	Key Technical Characteristics				Ref.
				Water Absorption (%)	Density (g/m^3)	Thermal Conductivity (W/m·K)	Compressive Strength (MPa)	
Water treatment sludge	Oakwood ash	Semi-dry pressing	1000	10–34	1.38–2	0.327–0.98	8–27	[58]
Clay	Water treatment sludge	Semi-dry pressing	800–1000	14–35	0.8–2.1	–	6–17	[59]
Clay	Waste marble, Sugarcane bagasse	Hand molding	900	12–22	–	–	7–18	[60]
Clay	Construction and demolition mix	Hand molding	700–900	13–27	1.22–1.5	–	1–23	[61]

4. Future Lines of Work and Limitations of This Study

In exploring the future prospects of utilizing natural zeolite and cigarette waste for the production of composite bricks, researchers aim to enhance sustainability and waste management practices. However, potential challenges and limitations include addressing the environmental impact of tobacco-related byproducts and ensuring the structural integrity of the resulting bricks. Furthermore, some extra investigation including freezing and thawing tests, leaching tests, and efflorescence tests could be necessary. As advancements continue, a critical focus will be placed on optimizing production processes to maximize thermal insulation properties while maintaining sufficient compressive strength. Balancing environmental benefits with practical considerations will be essential for the widespread adoption of this innovative approach.

5. Conclusions

This study focuses on the experimental investigation of composite ceramic bricks made from zeolite tuff and cigarette waste, aiming to improve the thermal insulation properties for non-load-bearing structural construction. A comprehensive range of physical and mechanical tests were conducted on bricks with varying percentages of cigarette waste (0–12 wt%). The experimental results yielded several key findings:

- The microstructural analysis demonstrated the critical role of sintering temperature in crystal phase formation, leading to the disintegration of smectite, clinoptilolite, illite/mica, and calcite, and the development of anorthite, which contributed to enhanced compressive strength.
- The inclusion of cigarette waste significantly impacted the brick properties, resulting in reduced interconnections between zeolite tuff grains and a lighter, more absorbent, and less resistant material.
- Water absorption increased with higher quantities of cigarette waste yet remained within the standard for mild weathering conditions.
- The compressive strength of the bricks decreased as cigarette waste was incorporated, although it still fell within the range specified for non-load-bearing bricks.
- Heat treatment at 1050 °C and 1150 °C promoted vitrification by facilitating condensation and pore-filling mechanisms, thereby reducing apparent porosity and forming closed pores.
- Moreover, the thermal conductivity of the samples containing cigarette waste was relatively low, ranging from 0.33 to 0.63 W/m·K for bricks sintered at 950 °C and 1050 °C, respectively, making them favorable for thermal insulation applications.

The incorporation of cigarette waste into the brick composition not only offers engineering benefits but also presents an opportunity for sustainable and eco-friendly production, contributing to landfill reduction and cleaner manufacturing processes.

Author Contributions: J.E.F.M.I.: Conceptualization, Methodology, Investigation, Formal analysis, Data curation, Writing—original draft. M.A.B.-M.K. and F.M.: Investigation, Formal analysis, and review & editing. I.K.: Supervision, Conceptualization, review & editing. All authors have read and agreed to the published version of the manuscript.

Funding: This research received no external funding.

Data Availability Statement: All data generated or analyzed during this study are included in this article.

Acknowledgments: We express our gratitude for the collaboration and support we received from our colleagues in the Departments of Ceramics and Polymer Engineering throughout the duration of this project.

Conflicts of Interest: The authors declare no conflicts of interest.

References

1. Ferronato, N.; Torretta, V. Waste Mismanagement in Developing Countries: A Review of Global Issues. *Int. J. Environ. Res. Public Health* **2019**, *16*, 1060. [CrossRef] [PubMed]
2. Salvia, G.; Zimmermann, N.; Willan, C.; Hale, J.; Gitau, H.; Muindi, K.; Gichana, E.; Davies, M. The Wicked Problem of Waste Management: An Attention-Based Analysis of Stakeholder Behaviours. *J. Clean. Prod.* **2021**, *326*, 129200. [CrossRef] [PubMed]
3. Bih, N.L.; Mahamat, A.A.; Chinweze, C.; Ayeni, O.; Bidossèssi, H.J.; Onwualu, P.A.; Boakye, E.E. The Effect of Bone Ash on the Physio-Chemical and Mechanical Properties of Clay Ceramic Bricks. *Buildings* **2022**, *12*, 336. [CrossRef]
4. Qamar, W.; Abdelgalil, A.A.; Aljarboa, S.; Alhuzani, M.; Altamimi, M.A. Cigarette Waste: Assessment of Hazard to the Environment and Health in Riyadh City. *Saudi J. Biol. Sci.* **2020**, *27*, 1380–1383. [CrossRef] [PubMed]
5. Ghasemi, A.; Golbini Mofrad, M.M.; Parseh, I.; Hassani, G.; Mohammadi, H.; Hayati, R.; Alinejad, N. Cigarette Butts as a Super Challenge in Solid Waste Management: A Review of Current Knowledge. *Environ. Sci. Pollut. Res.* **2022**, *29*, 51269–51280. [CrossRef] [PubMed]
6. Vanapalli, K.R.; Sharma, H.B.; Anand, S.; Ranjan, V.P.; Singh, H.; Dubey, B.K.; Mohanty, B. Cigarettes Butt Littering: The Story of the World's Most Littered Item from the Perspective of Pollution, Remedial Actions, and Policy Measures. *J. Hazard. Mater.* **2023**, *453*, 131387. [CrossRef] [PubMed]
7. Mohajerani, A.; Kadir, A.A.; Larobina, L. A Practical Proposal for Solving the World's Cigarette Butt Problem: Recycling in Fired Clay Bricks. *Waste Manag.* **2016**, *52*, 228–244. [CrossRef]
8. Kurmus, H.; Mohajerani, A. Recycling of Cigarette Butts in Fired Clay Bricks: A New Laboratory Investigation. *Materials* **2020**, *13*, 790. [CrossRef]
9. Maciel, L.A.R.; Loiola, R.L.; Holanda, J.N.F. Feasibility of Using Cigarette Butts Waste in Eco-Friendly Ceramic Roofing Tile. *SN Appl. Sci.* **2020**, *2*, 1–11. [CrossRef]
10. Kim, Y.; Cho, S.-H.; Lee, S.; Jung, S.; Chen, W.-H.; Kwon, E.E. Environmental Benefits from the Use of CO_2 in the Thermal Disposal of Cigarette Butts. *Environ. Res.* **2023**, *220*, 115217. [CrossRef]
11. Conradi, M.; Sánchez-Moyano, J.E. Toward a Sustainable Circular Economy for Cigarette Butts, the Most Common Waste Worldwide on the Coast. *Sci. Total Environ.* **2022**, *847*, 157634. [CrossRef] [PubMed]
12. George, M.; Khadtar, R. Review on Recycling of Microplastics in Cigarette Butts. In *IOP Conference Series: Earth and Environmental Science*; IOP Publishing: Bristol, UK, 2022; Volume 1084. [CrossRef]
13. Novotny, T.E.; Lum, K.; Smith, E.; Wang, V.; Barnes, R. Cigarettes Butts and the Case for an Environmental Policy on Hazardous Cigarette Waste. *Int. J. Environ. Res. Public Health* **2009**, *6*, 1691–1705. [CrossRef] [PubMed]
14. Araújo, M.C.B.; Costa, M.F. A Critical Review of the Issue of Cigarette Butt Pollution in Coastal Environments. *Environ. Res.* **2019**, *172*, 137–149. [CrossRef] [PubMed]
15. Kadir, A.A.; Mohajerani, A. Properties Improvement of Fired Clay Bricks Incorporating with Cigarette Butts. *Adv. Mater. Res.* **2012**, *535–537*, 1723–1730. [CrossRef]
16. Nazira Ab Karim, N.F.; Nabilah Sarbini, N.; Abdul Shukor Lim, N.H.; Syahrizal Ibrahim, I.; Aminuddin, E.; Rosseira Abu Talib, A. Thermal Insulation Properties of Organic and Inorganic Material in Clay Brick—A Review. In *IOP Conference Series: Earth and Environmental Science*; IOP Publishing: Bristol, UK, 2019; Volume 268. [CrossRef]
17. Kurmus, H.; Mohajerani, A. Energy Savings, Thermal Conductivity, Micro and Macro Structural Analysis of Fired Clay Bricks Incorporating Cigarette Butts. *Constr. Build. Mater.* **2021**, *283*, 122755. [CrossRef]
18. Ibrahim, J.E.F.M.; Tihtih, M.; Kurovics, E.; Gömze, L.A.; Kocserha, I. Innovative Glass-Ceramic Foams Prepared by Alkali Activation and Reactive Sintering of Clay Containing Zeolite (Zeolite-Poor Rock) and Sawdust for Thermal Insulation. *J. Build. Eng.* **2022**, *59*, 105160. [CrossRef]
19. Ibrahim, J.E.F.M.; Gömze, L.A.; Koncz-Horvath, D.; Filep, Á.; Kocserha, I. Preparation, Characterization, and Physicomechanical Properties of Glass-Ceramic Foams Based on Alkali-Activation and Sintering of Zeolite-Poor Rock and Eggshell. *Ceram. Int.* **2022**, *48*, 25905–25917. [CrossRef]

20. Kazantseva, L.K.; Yusupov, T.S.; Lygina, T.Z.; Shumskaya, L.G.; Tsyplakov, D.S. Foam Glass from Mechanoactivated Zeolite-Poor Rock. *Glass Ceram.* **2014**, *70*, 360–364. [CrossRef]
21. Farnood Ahmadi, P.; Ardeshir, A.; Ramezanianpour, A.M.; Bayat, H. Characteristics of Heat Insulating Clay Bricks Made from Zeolite, Waste Steel Slag and Expanded Perlite. *Ceram. Int.* **2018**, *44*, 7588–7598. [CrossRef]
22. Cobîrzan, N.; Thalmaier, G.; Balog, A.A.; Constantinescu, H.; Ceclan, A.; Nasui, M. Volcanic Tuff as Secondary Raw Material in the Production of Clay Bricks. *Materials* **2021**, *14*, 6872. [CrossRef]
23. Vakalova, T.V.; Revva, I.B. Use of Zeolite Rocks for Ceramic Bricks Based on Brick Clays and Clay Loams with High Drying Sensitivity. *Constr. Build. Mater.* **2020**, *255*, 119324. [CrossRef]
24. Ibrahim, J.E.F.M.; Kurovics, E.; Tihtih, M.; Gömze, L.A. Ceramic Bricks with Enhanced Thermal Insulation Produced from Natural Zeolite. *Pollack Period.* **2021**, *16*, 101–107. [CrossRef]
25. Gencel, O.; Sutcu, M.; Erdogmus, E.; Koc, V.; Cay, V.V.; Gok, M.S. Properties of Bricks with Waste Ferrochromium Slag and Zeolite. *J. Clean. Prod.* **2013**, *59*, 111–119. [CrossRef]
26. Erdogmus, E.; Sutcu, M.; Hossain, S.; Bayram, M.; Sarı, A.; Gencel, O.; Ozbakkaloglu, T. Effect of Molding Pressure and Firing Temperature on the Properties of Ceramics from Natural Zeolite. *Constr. Build. Mater.* **2023**, *402*, 132960. [CrossRef]
27. Ibrahim, J.E.F.M.; Gömze, L.A.; Kotova, O.B.; Shchemelinina, T.N.; Shushkov, D.A.; Ignatiev, G.V.; Anchugova, E.M. The Influence of Composition, Microstructure and Firing Temperature on the Density, Porosity, and Shrinkage of New Zeolite-Alumina Composite Material. *Epa.—J. Silic. Based Compos. Mater.* **2019**, *71*, 120–124. [CrossRef]
28. Cultrone, G.; Carrillo Rosua, F.J. Growth of Metastable Phases during Brick Firing: Mineralogical and Microtextural Changes Induced by the Composition of the Raw Material and the Presence of Additives. *Appl Clay Sci* **2020**, *185*, 105419. [CrossRef]
29. Wang, S.; Gainey, L.; Mackinnon, I.D.R.; Allen, C.; Gu, Y.; Xi, Y. Thermal Behaviors of Clay Minerals as Key Components and Additives for Fired Brick Properties: A Review. *J. Build. Eng.* **2023**, *66*, 105802. [CrossRef]
30. Vasić, M.V.; Radovanović, L.; Pezo, L.; Radojević, Z. Raw Kaolinitic–Illitic Clays as High-Mechanical-Performance Hydraulically Pressed Refractories. *J. Therm. Anal. Calorim.* **2023**, *148*, 1783–1803. [CrossRef]
31. García, V.J.; Zúñiga-Suárez, A.R.; Márquez, C.O.; Pérez, J.G.; Fernández-Martínez, F.; Hernández-Olivares, F. Strength Developing in Clay-Andesite Brick. *Mater. Sci. Appl.* **2016**, *7*, 403–420. [CrossRef]
32. Zhang, J.; Li, R.; Nie, D.; Zhang, Y. Preparation of Building Ceramic Bricks Using Waste Residue Obtained by Mutual Treatment of Electrolytic Manganese Residue and Red Mud. *Ceram. Int.* **2023**, *49*, 22492–22505. [CrossRef]
33. Andiç-Çakır, Ö.; Son, A.E.; Sürmelioğlu, S.; Tosun, E.; Sarıkanat, M. Improvement of Traditional Clay Bricks' Thermal Insulation Characteristics by Using Waste Materials. *Case Stud. Constr. Mater.* **2021**, *15*, e00560. [CrossRef]
34. Lawanwadeekul, S.; Srisuwan, A.; Phonphuak, N.; Chindaprasirt, P. Enhancement of Porosity and Strength of Clay Brick Fired at Reduced Temperature with the Aid of Corn Cob and Waste Glass. *Constr. Build. Mater.* **2023**, *369*, 130547. [CrossRef]
35. Phonphuak, N.; Saengthong, C.; Srisuwan, A. Physical and Mechanical Properties of Fired Clay Bricks with Rice Husk Waste Addition as Construction Materials. *Mater. Today Proc.* **2019**, *17*, 1668–1674. [CrossRef]
36. Chindaprasirt, P.; Srisuwan, A.; Saengthong, C.; Lawanwadeekul, S.; Phonphuak, N. Synergistic Effect of Fly Ash and Glass Cullet Additive on Properties of Fire Clay Bricks. *J. Build. Eng.* **2021**, *44*, 102942. [CrossRef]
37. Rukijkanpanich, J.; Thongchai, N. Burned Brick Production from Residues of Quarrying Process in Thailand. *J. Build. Eng.* **2019**, *25*, 100811. [CrossRef]
38. Chen, G.; Li, F.; Jing, P.; Geng, J.; Si, Z. Effect of Pore Structure on Thermal Conductivity and Mechanical Properties of Autoclaved Aerated Concrete. *Materials* **2021**, *14*, 339. [CrossRef] [PubMed]
39. Ali, S.A.; Fahmy, M.K.; Zouli, N.; Abutaleb, A.; Maafa, I.M.; Yousef, A.; Ahmed, M.M. Fabrication of Thermal Insulation Bricks Using Pleurotus Florida Spent Mushroom. *Materials* **2023**, *16*, 4905. [CrossRef] [PubMed]
40. Yaras, A. Combined Effects of Paper Mill Sludge and Carbonation Sludge on Characteristics of Fired Clay Bricks. *Constr. Build. Mater.* **2020**, *249*, 118722. [CrossRef]
41. Goel, G.; Vasić, M.V.; Katiyar, N.K.; Kirthika, S.K.; Pezo, M.; Dinakar, P. Potential Pathway for Recycling of the Paper Mill Sludge Compost for Brick Making. *Constr. Build. Mater.* **2021**, *278*, 122384. [CrossRef]
42. Brasileiro, C.T.; Conte, S.; Contartesi, F.; Melchiades, F.G.; Zanelli, C.; Dondi, M.; Boschi, A.O. Effect of Strong Mineral Fluxes on Sintering of Porcelain Stoneware Tiles. *J. Eur. Ceram. Soc.* **2021**, *41*, 5755–5767. [CrossRef]
43. Cultrone, G.; Sebastián, E.; Elert, K.; de la Torre, M.J.; Cazalla, O.; Rodriguez–Navarro, C. Influence of Mineralogy and Firing Temperature on the Porosity of Bricks. *J. Eur. Ceram. Soc.* **2004**, *24*, 547–564. [CrossRef]
44. Zaccaron, A.; de Souza Nandi, V.; Bernardin, A.M. Fast Drying for the Manufacturing of Clay Ceramics Using Natural Clays. *J. Build. Eng.* **2021**, *33*, 101877. [CrossRef]
45. Phonphuak, N.; Kanyakam, S.; Chindaprasirt, P. Utilization of Waste Glass to Enhance Physical-Mechanical Properties of Fired Clay Brick. *J. Clean. Prod.* **2016**, *112*, 3057–3062. [CrossRef]
46. Goel, G.; Kalamdhad, A.S. An Investigation on Use of Paper Mill Sludge in Brick Manufacturing. *Constr. Build. Mater.* **2017**, *148*, 334–343. [CrossRef]
47. Maza-Ignacio, O.T.; Jiménez-Quero, V.G.; Guerrero-Paz, J.; Montes-García, P. Recycling Untreated Sugarcane Bagasse Ash and Industrial Wastes for the Preparation of Resistant, Lightweight and Ecological Fired Bricks. *Constr. Build. Mater.* **2020**, *234*, 117314. [CrossRef]

48. Zhou, W.; Yang, F.; Zhu, R.; Dai, G.; Wang, W.; Wang, W.; Guo, X.; Jiang, J.; Wang, Z. Mechanism Analysis of Pore Structure and Crystalline Phase of Thermal Insulation Bricks with High Municipal Sewage Sludge Content. *Constr. Build. Mater.* **2020**, *263*, 120021. [CrossRef]
49. Eliche-Quesada, D.; Martínez-García, C.; Martínez-Cartas, M.L.; Cotes-Palomino, M.T.; Pérez-Villarejo, L.; Cruz-Pérez, N.; Corpas-Iglesias, F.A. The Use of Different Forms of Waste in the Manufacture of Ceramic Bricks. *Appl. Clay Sci.* **2011**, *52*, 270–276. [CrossRef]
50. Muñoz, P.; Letelier, V.; Bustamante, M.A.; Marcos-ortega, J.; Sepúlveda, J.G. Assessment of Mechanical, Thermal, Mineral and Physical Properties of Fired Clay Brick Made by Mixing Kaolinitic Red Clay and Paper Pulp Residues. *Appl. Clay Sci.* **2020**, *198*, 105847. [CrossRef]
51. Riaz, M.H.; Khitab, A.; Ahmad, S.; Anwar, W.; Arshad, M.T. Use of Ceramic Waste Powder for Manufacturing Durable and Eco-Friendly Bricks. *Asian J. Civ. Eng.* **2020**, *21*, 243–252. [CrossRef]
52. Sutcu, M.; Alptekin, H.; Erdogmus, E.; Er, Y.; Gencel, O. Characteristics of Fired Clay Bricks with Waste Marble Powder Addition as Building Materials. *Constr. Build. Mater.* **2015**, *82*, 1–8. [CrossRef]
53. Pacheco-Torgal, F.; Lourenco, P.B.; Labrincha, J.; Chindaprasirt, P.; Kumar, S. (Eds.) *Eco-Efficient Masonry Bricks and Blocks: Design, Properties and Durability*; Woodhead Publishing: Cambridge, UK, 2014; ISBN 9780857090287.
54. Ibrahim, J.E.F.M.; Tihtih, M.; Basyooni, M.A.; Kocserha, I. Innovative Sustainable Ceramic Bricks: Exploring the Synergy of Natural Zeolite Tuff and Aluminum Dross. *Constr. Build. Mater.* **2023**, *409*, 133947. [CrossRef]
55. Ibrahim, J.E.F.M.; Kotova, O.B.; Sun, S.; Kurovics, E.; Tihtih, M.; Gömze, L.A. Preparation of Innovative Eco-Efficient Composite Bricks Based on Zeolite-Poor Rock and Hen's Eggshell. *J. Build. Eng.* **2022**, *45*, 103491. [CrossRef]
56. Hei, F.; Liu, Q.; Zhao, G.; Ou, J.; Xu, F. Preparation and Characteristics of the Fired Bricks Produced from Polyaluminum Chloride Slag and Glass Powder. *Appl. Sci.* **2023**, *13*, 1989. [CrossRef]
57. Balog, A.A.; Constantinescu, H. Fired Tone Waste Addition for Fired Clay Bricks. *Materials* **2022**, *15*, 1–12.
58. Harja, M.; Gencel, O.; Sarı, A.; Sutcu, M.; Erdogmus, E.; Hekimoglu, G. Production and Characterization of Natural Clay-Free Green Building Brick Materials Using Water Treatment Sludge and Oak Wood Ash. *Arch. Civ. Mech. Eng.* **2022**, *22*, 79. [CrossRef]
59. Abbas, S.; Baig, A.; Hameed, R.; Kazmi, S.M.S.; Munir, M.J.; Shaukat, S. Manufacturing of Clay Bricks Using Hybrid Waste Marble Powder and Sugarcane Bagasse Ash: A Sustainable Building Unit. *Sustainability* **2023**, *15*, 14692. [CrossRef]
60. Ahmadi, M.; Hakimi, B.; Mazaheri, A.; Kioumarsi, M. Potential Use of Water Treatment Sludge as Partial Replacement for Clay in Eco-Friendly Fired Clay Bricks. *Sustainability* **2023**, *15*, 9389. [CrossRef]
61. Dubale, M.; Vasić, M.V.; Goel, G.; Kalamdhad, A.; Singh, L.B. Utilization of Construction and Demolition Mix Waste in the Fired Brick Production: The Impact on Mechanical Properties. *Materials* **2023**, *16*, 262. [CrossRef]